A Novel Real-Time Error Adjustment Method with Considering Four Factors for Correcting Hourly Multi-satellite Precipitation Estimates

Hanqing Chen, Bin Yong, Jonathan J. Gourley, Debao Wen, Weiqing Qi, Kun Yang

***Abstract*—High-accuracy near-real-time satellite precipitation estimates (SPEs) provide an opportunity for hydrometeorologists to improve the forecasting of extreme events, such as flood, landslide, tropical cyclone and other extreme events, at the large scale. However, the currently operational near-real-time SPEs still have larger errors and uncertainties. In this study, we found that there exists a clear relationship of spatial plane function (SPF) between retrieval errors of SPEs and four crucial factors including topography, seasonality, climate type and rain rate. Based on this finding, we proposed a novel error adjustment method to correct the near-real-time hourly Global Satellite Mapping of Precipitation (GSMaP-NRT) estimates in real time. The new satellite precipitation dataset, namely ILSF-RT, was then inter-compared with the latest near-real-time GSMaP product suite (i.e., GSMaP-NRT and GSMaP-Gauge-NRT). Verification results show that the proposed method can effectively reduce the retrieval errors of GSMaP-NRT for various terrains and rain rates over different seasons and climate type areas. The new ILSF-RT even exhibits a general improvement over the GSMaP-Gauge-NRT estimates. Furthermore, one important merit of the new method is that it can perform rather well in validation even not much historical data were applied as training samples in calibration, for example, during the generation of ILSF-RT, only 45 data pairs of satellite retrievals and ground observations were used for winter season over Chinese arid areas. However, the results of bias score show that the current method seems unsuitable to adjust the rainfall events with higher rain rates (>= 1mm hr^{-1}), which needs to be further improved.**

***Index Terms*—Error correction, precipitation, crucial factors, ILSF-RT, real time, mainland China.**

I. Introduction

With the rapid development of remote sensing technique in the last 20 years, the retrieval information from various satellite sensors becomes a reliable data source of obtaining areal precipitation estimates over large scales and even globe. Although the satellite-based precipitation estimates are indirect, the high frequency and broad coverage make them uniquely complementary to conventional rain gauge networks and weather radars [1], [2]. Also, the satellite-based precipitation estimates provide an opportunity for both hydrologists and meteorologists to improve the forecasting of extreme events, such as flood warning, landslide detection, typhoon monitoring, and drought diagnosis, at the large scale [3]-[6]. In practice, the near real-time satellite precipitation products (SPPs) are more appropriate for these hydrometeorological predictions relative to post-real-time research-quality SPPs. However, the near real-time SPPs normally have larger errors and uncertainties than the post-real-time products [7]. Therefore, it is important to develop effective error correction methods for further improving the data accuracy of mainstream SPPs in real time, which will significantly enhance their application potentials especially for natural hazard warning. This is also one of the primary science objectives of the Global Precipitation Measurement (GPM) mission (https://www.nasa.gov/mission_pages/GPM/science/index.html).

The scientific understanding of error features of satellite precipitation estimates is essential to establish the error adjustment model (EAM) in correction methods [8]. Currently, a considerable number of literatures have revealed the error characteristics of SPPs at regional [9]-[15] or global [5], [16], [17] scales. Some other studies found that the retrieval errors of satellite precipitation are closely related to topography [18]-[21], seasonality [22]-[24], climate types [25], [26], and rain rates [27], [28]. However, a comprehensive investigation with regard to the relationships between retrieval errors and four factors (i.e., topography, seasonality, climate type, and rain rate) is still lacking. This limitation hinders establishing a fairly trustworthy EAM, which can thoroughly consider various geographic and climatic factors to effectively reduce the errors of satellite precipitation estimates. By analyzing the error components of GPM-based passive microwave and infrared sensors, on the first time, we comprehensively revealed the dependency of retrieval errors of satellite precipitation on the

This work was supported by the National Key Research and Development Program of China (No. 2018YFA0605402), the National Natural Science Foundation of China (Nos. 51979073 and 42074030), and the China Postdoctoral Science Foundation (No. 2021M700923). *Corresponding author: Bin Yong.*

Hanqing Chen and Debao Wen are with the School of Geography and Remote Sensing, Guangzhou University, Guangzhou 510006, China, and Hanqing Chen is also with the State Key Laboratory of Hydrology-Water Resources and Hydraulic Engineering, Hohai University, Nanjing 210098, China.

Bin Yong and Weiqing Qi are with the State Key Laboratory of Hydrology-Water Resources and Hydraulic Engineering, Hohai University, Nanjing 210098, China (e-mail: yongbin@hhu.edu.cn).

Jonathan J. Gourley is with NOAA/National Severe Storms Laboratory, Norman, OK 73072, USA.

Kun Yang is with the Department of Earth System Science/Ministry of Education Key Laboratory for Earth System Modeling, Tsinghua University, Beijing, China.

topography, season, and climate type over mainland China [29]. Furthermore, a power function relationship between the retrieval errors and the logarithm of rain rates was subsequently proposed in the extended study [7]. As a continuation of previous works, this study primarily aims at establishing an effective EAM to correct the hourly near-real-time global satellite mapping of precipitation (GSMaP-NRT) by analyzing the function relationships between satellite retrieval errors and multiple factors in details.

In practice, many previous literatures have proposed various correction methods to improve the accuracy of the near real-time SPPs for enhancing their potentials in natural hazard forecasting [30]-[38]. However, these correction methods suffer from different defects: (1) some methods strongly depend on the ground observations in real time and their effectiveness is also closely related to the observed accuracy [31], [32], [38]; (2) some methods employed the satellite-derived soil moisture products to correct satellite precipitation estimates in real time, but these ways may introduce new error sources and degrade the retrieval quality of original SPPs [33], [37]; (3) others only selected single or few factors but neglected some crucial ones associated with retrieval errors, leading to the fundamental algorithmic defects in establishing the EAMs [35], [36]; (4) some real-time error correction methods work for only reducing systematic error [30]-[32], [34], but the major error component of current satellite products is random error [8]. Merging different precipitation products is an effective way to enhance the quality of SPPs [39]-[43]. However, it cannot correct satellite precipitation estimates in real time.

Chen et al. [7] found that there exist substantial errors and larger uncertainties in the currently operational near real-time satellite precipitation products, such as GSMaP-NRT [44], GSMaP-MVK (Global Satellite Mapping of Precipitation Microwave-IR Combined Product) [45], IMERG-Early and IMERG-Late (Integrated Multi-satellite Retrievals for GPM Early and Late runs) [46], and PERSIANN-CCS (Precipitation Estimation from Remotely Sensed Information using Artificial Neural Networks Cloud Classification System) [47], [48]. Among them, GSMaP-NRT is one of the standard GPM-based SPPs, which can be widely applied for monitoring various natural disasters. To further improve the retrieval accuracy, the GSMaP team of Japan Aerospace Exploration Agency (JAXA) also developed another near real-time product, namely the gauge-calibrated GSMaP-NRT (i.e., GSMaP-Gauge-NRT) by integrating the Climate Precipitation Center unified gauge-based precipitation data (CPCU; [49]). However, a preliminary assessment indicated that this gauge-adjusted precipitation product still has relatively large errors and needs to be revisited in the future studies [50].

Consequently, here we proposed a novel real-time error adjustment method that considers four impacting factors to precipitation errors to correct for the hourly GSMaP-NRT precipitation estimates in real time. The improved ill-posed least squares (ILS) algorithm was applied in this new method. We expect that this work can help data developers to upgrade the present correction methods, and provide end-users a useful postprocessing step for available near real-time products when the high-quality satellite precipitation estimates are required in their hydrometeorological applications.

II. DATASETS

Two GPM-based hourly satellite precipitation estimates, including GSMaP-NRT and GSMaP-Gauge-NRT, were utilized in this study. The processing algorithm of the near real-time GSMaP suite mainly includes the following five steps: (1) the Dual-frequency phased array Precipitation Radar (DPR) data were used to calibrate passive microwave (PMW) retrievals; (2) the morphing technique adopting the cloud movements computed by two successive infrared images was used to generate the precipitation estimates from PMW retrievals. Note that only temporarily forward cloud movement was used in this step; (3) a Kalman filter method was applied to refine precipitation rates from morphing technique; (4) a microwave-IR merging module was applied to produce the hourly global precipitation estimates in near real time, namely GSMaP-NRT; (5) GSMaP-NRT was adjusted by the error parameters derived from the historical daily-daily data pairs of satellite retrievals (GSMaP-NRT itself) and gauge observations (i.e., CPCU) to generate the gauge-adjusted product GSMaP-Gauge-NRT.

In our study, the hourly GSMaP-NRT was first corrected by the proposed method to produce a set of new precipitation product ILSF-RT, which was then intercompared with both GSMaP-NRT and GSMaP-Gauge-NRT to validate the new method. An observation network of over 30,000 conventional rain gauges covering mainland China (Fig.1a) was employed to calibrate and validate the error adjustment models in the new method. This reference dataset has a high spatiotemporal resolution (hourly, 0.1º; [32]). Here, we selected one complete year of 2015 with GSMaP-NRT and ground observations for calibration and two years of three datasets (two near real-time GSMaP products and gauged observations), from April 2017 to March 2019, for validation, considering the GSMaP-Gauge-NRT V7 data available starting from April 2017.

III. METHODOLOGY

A. Real-time error correction method

The EAM that can accurately describe the error features of satellite retrievals is essential to customize error correction methods. Our previous studies have found that the errors of satellite-based precipitation estimates are closely related to four crucial factors, i.e., seasonality, topography, climate type, and rain rate [7], [8], [29]. However, the comprehensive relationships between satellite retrieval errors and these four factors are still not investigated, and the expected EAM was also not established. As an extension of our previous works, this study attempts to comprehensively consider four crucial factors associated with retrieval errors and effectively correct the near real-time multi-satellite precipitation estimates by the EAM derived from historical satellite-gauge data pairs.

In the new correction method, we design a better expression for topography using the standard deviation of elevation (SDE, see Fig.1b) to substitute the original average elevation.

Additionally, we continue to adopt the original division scheme of climate types (Fig. 1a) proposed in Chen et al. [29], which divides mainland China into four climate types (humid, semi-humid, semi-arid, and arid).

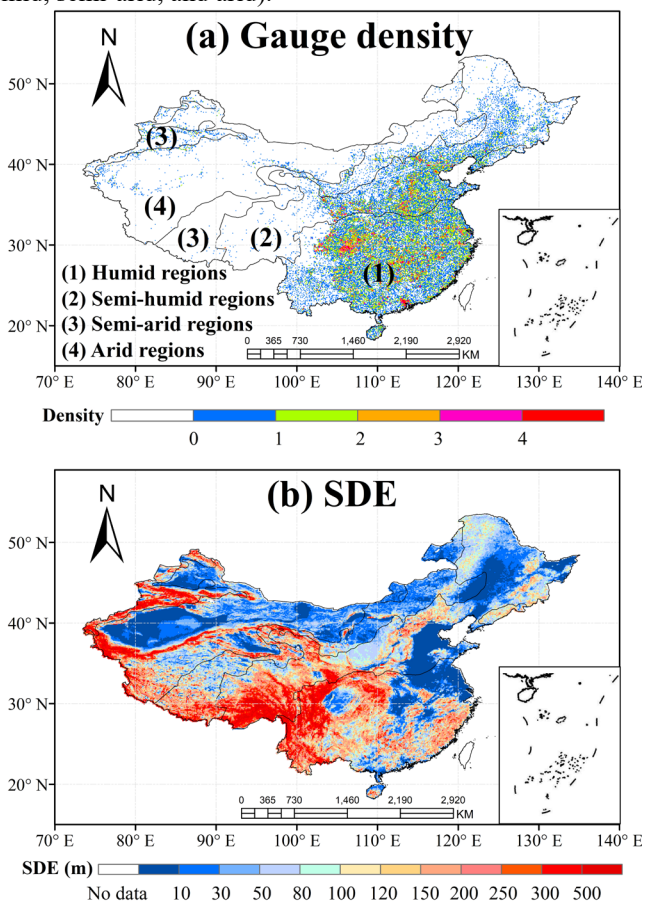

Fig. 1. (a) Spatial map of rain gauges (over 30,000) and four climate types (humid, semi-humid, semi-arid, arid) used in this study, (b) map of the standard deviation of elevation (SDE), over mainland China.

The retrieval errors (E) can be simply calculated by satellite rain rate (S) minus ground observations (G). The specific equation can be written as:

$$\mathrm{E} = \mathrm{S} - \mathrm{G} \tag{1}$$

To clearly demonstrate the links between E and two crucial factors (i.e., topography and rain rate), we divide satellite-gauge datasets into 16 categories according to four seasons and four climate types over mainland China. Fig.2 shows the 3-D views of E as a function of SDE and rain rate in the GSMaP-NRT estimates. Interestingly, it is found that there exists an apparent spatial plane function relationship between the errors of GSMaP-NRT and two crucial factors (i.e., topography and rain rate) for all the sixteen categories. Based on such function relationships, we established sixteen different EAMs to adjust the GSMaP-NRT precipitation estimates. The main formulae of proposed EAMs can be defined as:

$$\mathrm{E}_{i,j} = \mathrm{a}_{i,j} * \mathrm{S} + \mathrm{b}_{i,j} * \mathrm{SDE} + \mathrm{c}_{i,j} \tag{2}$$

where $\mathrm{a}_{i,j}, \mathrm{b}_{i,j}$, and $\mathrm{c}_{i,j}$ are the key parameters of the EAMs. The subscripts i (i = 1, 2, 3, 4) and j (j = 1, 2, 3, 4) represent the four seasons (i.e., spring, summer, autumn, and winter) and the four climate types (i.e., humid, semi-humid, semi-arid, and arid), respectively. By substituting Eq. (1) into Eq. (2), the sixteen function relationships in the proposed EAMs can be expressed as:

$$G_{i,j} = \left(1 - \mathrm{a}_{i,j}\right)S - \mathrm{b}_{i,j}SDE - \mathrm{c}_{i,j} \tag{3}$$

Eq. (3) can be transformed to a simple formula:

$$G = AX \tag{4}$$

where $A = [\mathrm{S}, \mathrm{SDE}, 1]$, $X = [1 - \mathrm{a}, -\mathrm{b}, -\mathrm{c}]^T$. Compared with those error adjustment modules in prior literatures, the new EAM proposed here can better depict the relationships between the retrieval errors of satellite precipitation and the four crucial factors (seasonality, topography, climate type, and rain rate).

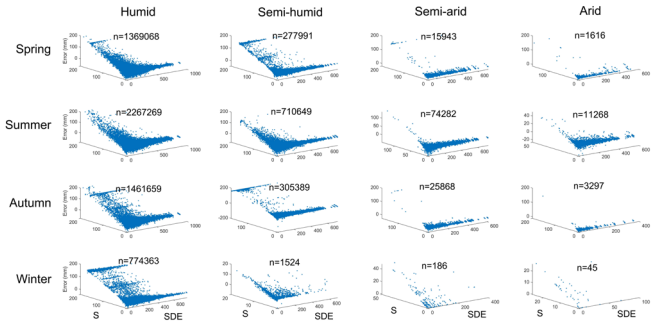

Fig. 2. Scatter plots (3-D views) of retrieval errors of GSMaP-NRT as a function of topography (SDE) and satellite rain rate (S) for 16 categories according to four seasons (spring, summer, autumn, winter) and four climate types (humid, semi-humid, semi-arid, arid) over mainland China. Note that n indicates the sample sizes for different cases.

The key parameter (X) for above Eq. (4) can be normally calculated by the least square method. The parameter estimates are denoted by $\hat{X}_{LS}$, which can be computed as:

$$\hat{X}_{LS} = (A^T A)^{-1} A^T G \tag{5}$$

However, in our numerical experiments, we found that the condition number of matrix $\mathrm{A}^T A$ is beyond 1,000, which causes its determinant close to zero, resulting to the matrix $\mathrm{A}^T A$ seriously ill-conditioned. This leads to instability of calculating solution of least square method. Therefore, an ILS approach was applied to perform the parameter estimates of X for the sixteen EAMs. The equation of the $\hat{X}_{ILS}$can be expressed as:

$$\hat{X}_{ILS} = (A^T A + \alpha I)^{-1} A^T G \tag{6}$$

where α denotes ridge parameter, which can be calculated by L-curve method (refer to Hansen et al. [51] for more details); while the symbol I is an identity matrix. By the item of αI, Eq. (6) can reduce the degree of ill condition for the matrix $A^T A$ and provide reliable parameter estimates for the EAMs.

Through the preliminary data analysis before EAM construction, we found that some outliers, which might be caused by the larger errors of satellite estimates and/or gauge observations, are mixed in the training samples. This will result in a serious deviation between the parameter estimate of the ILS and its 'truth value'. Consequently, a robust ILS (RILS) method was proposed to remove the outliers before starting the aforementioned parameter estimation for the sixteen EAMs. The procedure of RILS-based outlier elimination mainly includes the following four steps:

1) the ILS method was used to compute the initial parameter estimates of the sixteen EAMs (i.e., Eq. (2)).
2) the distances (d) between the selected points and the fitting plane were calculated by substituting

parameter estimates, S, SDE, and E into the following equation:

$$d = \frac{|S\times\hat{a}+SDE\times\hat{b}-E+\hat{c}|}{\sqrt{\hat{a}^2+\hat{b}^2+1}} \quad (7)$$

3) thus, the standard deviation of the distance (σ) could be worked out using the following formula pair:

$$\begin{cases} \bar{d} = \frac{1}{n}\sum_{i=1}^{n} d_i \\ \sigma = \sqrt{\frac{\sum_{i=1}^{n}(d_i-\bar{d})^2}{n-1}} \end{cases} \quad (8)$$

4) if $d_i < 3\sigma$, the corresponding training sample will be retained to join the following training. Otherwise, it will be eliminated as an outlier.

Next, the remaining samples will be directly applied to train the EAMs, which then generate the new precipitation product ILSF-RT. Fig. 3 displays the entire flowchart of the new method and its main processing steps are briefly described as follows:

1) calculating the errors of satellite estimates. One complete year of both GSMaP-NRT (S) and ground observations (G) were used as the training samples in calibration. The errors between S and G were computed by Eq. (1).
2) establishing sixteen EAMs based on the analyses of four crucial factors. All the satellite-gauge data pairs were spatiotemporally separated into 16 categories over mainland China according to four seasons and four climate types. Thus, 16 EAMs of retrieval errors as a spatial plane function of topography (SDE) and satellite rain rate (S) were established (refer to Fig. 2 and Eq. (2)).
3) removing the outliers. This step has been clearly explained in above RILS-based outlier elimination.
4) calibrating the model parameters of EAMs. The ILS method was employed to compute the parameter estimates of sixteen EAMs (i.e., Eq. (4)).
5) generating the new precipitation product ILSF-RT. The new method primarily adopts the ILS method to solve the parameter estimates of the EAMs that consider four factors, and then the errors and biases of GSMaP-NRT are reduced based on Eq. (4) and Eq. (6). Finally, ILSF-RT product was comprehensively intercompared with GSMaP-NRT and GSMaP-Gauge-NRT over mainland China for validation using various evaluation indices.

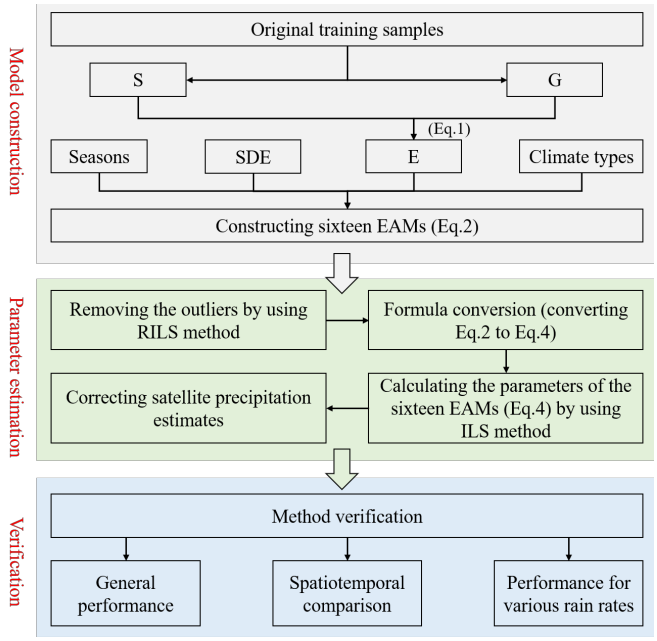

Fig. 3. The flowchart of the new real-time error correction method.

B. *Statistical indices in evaluation*

To quantify the performance of the new proposed method, we used seven statistical indices including correlation coefficient (CC), root mean squared error (RMSE), normalized root mean squared error (NRMSE), relative bias (RBIAS), and three types of error components (hit bias, miss bias, and false bias). The CC was used to denote the agreements between evaluated precipitation product and ground observations. RMSE describes the absolute errors of evaluated precipitation datasets. As a supplement metric, NRMSE was used to assess the accuracy of evaluated precipitation products in different rain rates. RBIAS and three independent components were used to measure the systematic biases of precipitation estimates. The corresponding formulae of all above statistical indices are provided in Table I.

TABLE I
NINE EVALUATION SCORES USED IN THIS STUDY FOR VERIFYING THE PROPOSED APPROACH.

Evaluation scores	Equation	Perfect value
Correlation Coefficient (CC)	$CC = \frac{\sum_{i=1}^{n}(G_i-\bar{G})(S_i-\bar{S})}{\sqrt{\sum_{i=1}^{n}(G_i-\bar{G})^2}\times\sqrt{\sum_{i=1}^{n}(S_i-\bar{S})^2}}$	1
Root Mean Squared Error (RMSE)	$RMSE = \sqrt{\frac{1}{n}\sum_{i=1}^{n}(S_i-G_i)^2}$	0
Normalized Root Mean Squared Error (NRMSE)	$NRMSE = \frac{\sqrt{\frac{1}{n}\sum_{i=1}^{n}(S_i-G_i)^2}}{\bar{G}}$	0
Relative Bias (RBIAS)	$BIAS = \frac{\sum_{i=1}^{n}(S_i-G_i)}{\sum_{i=1}^{n}G_i}\times 100\%$	0
Hit Bias (HB)	$HB = \frac{\sum_{i=1}^{n}(S_{H_i}-G_{H_i})}{\sum_{i=1}^{n}G}\times 100\%$	0
Miss Bias (MB)	$MB = \frac{\sum_{i=1}^{n}(-G_{M_i})}{\sum_{i=1}^{n}G}\times 100\%$	0
False Bias (FB)	$FB = \frac{\sum_{i=1}^{n}(S_{F_i})}{\sum_{i=1}^{n}G}\times 100\%$	0

IV. RESULTS

A. General performance

Table II lists the statistical summary of GSMaP-NRT, GSMaP-Gauge-NRT and ILSF-RT for four seasons over mainland China during the calibration and validation periods. Generally, almost all the statistical indices show a significant improvement of ILSF-RT over GSMaP-NRT and GSMaP-Gauge-NRT, only except for slightly lower CC values than those of GSMaP-Gauge-NRT. The evident improvement of GSMaP-Gauge-NRT product in CC score might benefit from daily-scale correction. Relative to original GSMaP-NRT, the corrected ILSF-RT still exhibits a clear improvement in correlation for the calibration and validation periods. As for other two evaluation scores (RMSE and RBIAS), ILSF-RT that has the smallest errors and biases for most cases apparently outperforms both GSMaP-NRT and GSMaP-Gauge-NRT. Moreover, the new method seems to be more effective in those autumn and winter months. Taking the autumn of validation period for instance, the value of RMSE remarkably decreases from 1.41 mm hr^{-1} before correction to only 0.65 mm hr^{-1} after correction, a 53.9% drop. Also, the value of RBIAS decreases from 37.2% of GSMaP-NRT and 40.18% of GSMaP-Gauge-NRT to -15.75% of ILSF-RT in winter. Overall, we can conclude that the new proposed method can substantially improve the data accuracy of hourly GSMaP-NRT estimates and even performs better than the gauged adjustment scheme employed in GSMaP-Gauge-NRT.

TABLE II
THE SUMMARY OF THE THREE EVALUATION INDICES (I.E., CC, RMSE, AND RBIAS) FOR THE THREE PRODUCTS (I.E., GSMAP-NRT, GSMAP-GAUGE-NRT, AND ILSF-RT) OVER FOUR SEASONS FOR THE CALIBRATION AND VALIDATION PERIODS.

Period	Metric results	Spring			Summer			Autumn			Winter		
		GSMaP-NRT	GSMaP-Gauge-NRT	ILSF-RT	GSMaP-NRT	GSMaP-Gauge-NRT	ILSF-RT	GSMaP-NRT	GSMaP-Gauge-NRT	ILSF-RT	GSMaP-NRT	GSMaP-Gauge-NRT	ILSF-RT
Calibration	CC	0.26	0.42	0.41	0.41	0.45	0.42	0.18	0.36	0.34	0.16	0.41	0.37
	RMSE (mm)	1.7	0.9	0.7	1.2	1.1	1.0	1.6	0.9	0.7	1.7	0.7	0.3
	RBIAS (%)	33.2	7.1	-7.5	-1.5	1.5	1.2	9.0	12.3	-9.4	61.0	36.4	-21.5
Validation	CC	0.32	0.40	0.38	0.33	0.38	0.37	0.22	0.38	0.32	0.13	0.30	0.30
	RMSE (mm)	1.3	0.9	0.7	1.8	1.4	1.2	1.4	0.9	0.7	1.1	0.6	0.3
	RBIAS (%)	51.4	18.2	16.0	12.8	9.1	-7.7	20.1	37.9	1.5	37.3	40.2	-15.8

The boxplots of the RMSE and RBIAS indicators were used to further analyze and compare the performance of three SPPs, as shown in Figs.4-5. Fig.4 illustrates the numerical distribution of RMSE for four seasons and four different climate types. Generally, ILSF-RT with relatively lower RMSE outperforms other two SPPs for all the cases. In particular, ILSF-RT exhibits significant improvements for cold seasons and arid areas during both the calibration and validation periods. Additionally, the boxplot results of RBIAS in Fig. 5 also suggest similar results in that ILSF-RT with lower relative biases has the best performance among three evaluated SPPs, although larger RBIAS values appear in winter season and arid areas. This might be attributed to two major reasons: (1) fewer precipitation events and smaller rainfall amounts during the cold season, and (2) larger uncertainties induced by using sparse in-situ observations over arid areas in the evaluation [6], [29]. In summary, above statistical analysis from two different indices shows the new proposed method can effectively reduce the seasonal and climatic retrieval errors of GSMaP-NRT to some extent and substantially improve its data accuracy.

B. Spatiotemporal comparison

The spatial maps of the differences of RMSE between GSMaP-Gauge-NRT and GSMaP-NRT and between ILSF-RT and GSMaP-NRT for different seasons give a clear indication of where these datasets are performing better or worse (see Fig. 6). During the calibration period, one can see that the differences of RMSE between GSMaP-Gauge-NRT and GSMaP-NRT are below 0% over most areas of humid areas, meaning that the error correction method employed in GSMaP-Gauge-NRT product reduces the accuracy of the original GSMaP-NRT product in such areas. As for the new method, we found that the differences of RMSE between ILSF-RT and GSMaP-NRT are exceeding 0% over most areas of mainland China, suggesting that the new error correction method improves the accuracy of the original GSMaP-NRT to some extent. Especially, the new method enhances the accuracy of the original GSMaP-NRT over 80% in Sichuan province where has multiple topography classes. Besides, the accuracy improvement of the new error correction method displays seasonal and regional features.

During the validation period, similar to the calibration period, the differences of RMSE between GSMaP-Gauge-NRT and GSMaP-NRT are below 0% over most areas of humid areas, especially for autumn and winter seasons. This means that the error correction method used in GSMaP-Gauge-NRT degrades the performance of the original GSMaP-NRT product. Oppositely, the new proposed error correction method improves the performance of the original GSMaP-NRT evidently over most areas of mainland China due to the corresponding RMSE difference values exceeding 0%. It should be noted that the new error correction method also improved the accuracy of GSMaP-NRT more than 80% in Sichuan province where has multiple terrains. This further tests

the ability of the new method on reducing the rainfall errors of GSMaP-NRT in complex terrain areas, which is chiefly attributed to the impact of topography information having been considered in our correction method. In summary, the spatial analyses from Fig. 6 demonstrates that the new method effectively reduce the retrieval errors of GSMaP-NRT for various terrains and over different seasons and climate areas and ILSF-RT generally exhibits the best performance among three evaluation products.

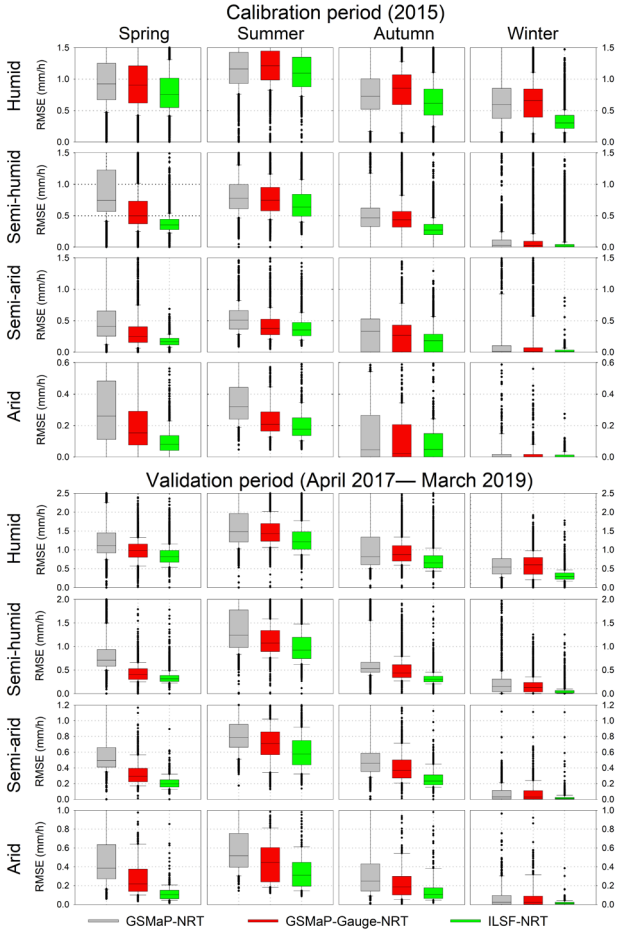

Fig. 4. The boxplots of the RMSE score for the three products (i.e., GSMaP-NRT (grey), GSMaP-Gauge-NRT (red), and ILSF-RT (green)) in four seasons (i.e., spring (first column), summer (second column), autumn (third column), and winter (fourth column)) over four climate types (i.e., humid (first line), semi-humid (second line), semi-arid (third line), and arid (fourth line)). Note that some boxplots are not represented entirely because of their larger ranges.

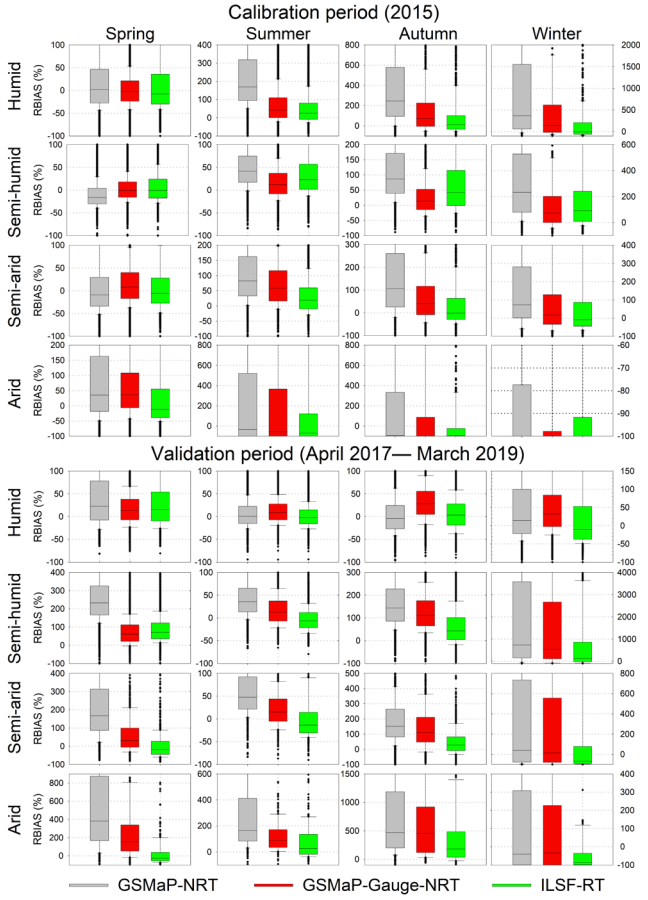

Fig5. As in Fig. 4 but for RBIAS.

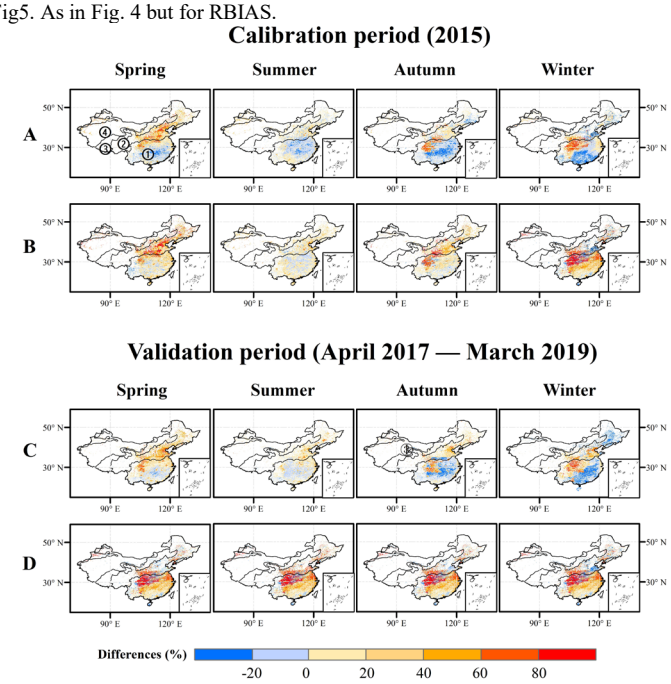

Fig. 6. Spatial maps of RMSE differences (lines A and C) between GSMaP-Gauge-NRT and GSMaP-NRT and (lines B and D) between ILSF-RT and GSMaP-NRT for four seasons: spring (first column), summer (second column), autumn (third column), and winter (fourth column). Note that ①, ②, ③, and ④ represent humid, semi-humid, semi-arid, and arid type areas, respectively.

Fig. 7 exhibits the comparison of time series of RMSE for these three evaluated products during the calibration and validation periods. Generally speaking, both ILSF-RT and

GSMaP-Gauge-NRT effectively reduce the error and bias of original GSMaP-NRT. But apparently, ILSF-RT exhibits the best performance among three products, suggesting that the new proposed method might benefit to enhance the application potentials of GPM-based satellite precipitation estimates in real-time natural hazard warning.

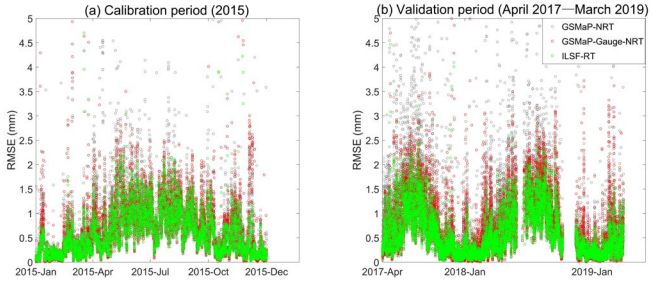

Fig. 7. Time series of RMSE for the three products (i.e., GSMaP-NRT, GSMaP-Gauge-NRT, and ILSF-RT) over the entire mainland China for the calibration and validation periods. Note that the blank parts indicate that the benchmark is missing.

C. Performance for different rain rates

To help diagnose the performance of ILSF-RT at different rain rates, the hourly rainfall events were classified by setting fixed thresholds of 0.2, 0.4, 0.6, 1, 2, and 5 mm as documented in Chen et al. [7]. We found that the values of RMSE metric increase with increasing rain rates, which is not conducive to the performance comparisons among different products in different precipitation intensities. Therefore, we selected the normalized RMSE (NRMSE) to replace RMSE metric in investigating the accuracy of the three products in various rain rates. To ensure the reliability of the verification results, the sample sizes of various rain rates for both calibration and validation periods are given in Figs. 8a-b. It can see that the sample sizes of all the categories are over 2.0e+6, suggesting that these sufficient samples support the reliability of the results. Besides, the intensity distributions of errors and biases of three hourly precipitation products, including NRMSE and RBIAS, are shown in Figs.8c-d.

The intensity distribution of hourly rainfall amount provides unique insights into the error dependence on rain rates. Fig. 8c and 8d clearly show that ILSF-RT has relatively lower values of NRMSE than GSMaP-NRT and GSMaP-Gauge-NRT at most ranges of rain rates except for over 5 mm hr^{-1}, suggesting that the correction method chiefly improve the data quality of GSMaP-NRT at low-medium rain rates. As for RBIAS metric, ILSF-RT has smaller values of RBIAS than GSMaP-NRT and GSMaP-Gauge-NRT at the rain rates less than 1 mm hr^{-1}, while relatively larger RBIAS over 1 mm hr^{-1} (Fig. 9c), during both calibration and validation periods. But it is worth noting that GSMaP-Gauge-NRT also exhibits larger RBIAS than GSMaP-NRT at the range during the validation period. The results imply that the gauge-based correction methods applied in both ILSF-RT and GSMaP-Gauge-NRT have limitations at high rain rates. This might be due to the overcorrection of the error adjustment methods, leading to reducing the performance of original satellite product in RBIAS score at such rain rates. Based on the results of the two scores (i.e., NRMSE and RBIAS) shown in Fig. 8, it can be concluded that positive and negative biases in GSMaP-NRT cancel each other to some degree because the absolute errors of GSMaP-NRT seems not better than those of two gauge-adjusted products over the medium-high rain rates (>1 mm hr^{-1}).

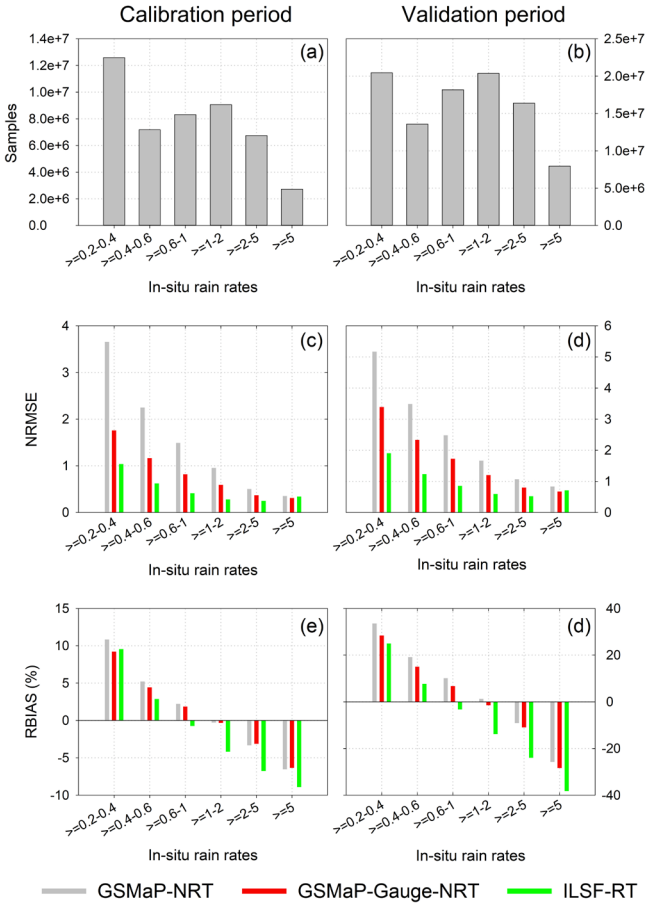

Fig. 8. (a-b) The sample sizes of six rain rate categories for the calibration and validation periods, (c-d) the NRMSE of the three products (i.e., GSMaP-NRT, GSMaP-Gauge-NRT, and ILSF-RT) at 0.1° spatial and hourly temporal resolution under different rain rates, (e-d) the RBIAS of the three products (i.e., GSMaP-NRT, GSMaP-Gauge-NRT, and ILSF-RT) at 0.1° spatial and hourly temporal resolution under different rain rates.

V. DISCUSSION

A. Which error components are effectively corrected by the new method?

Performance evaluation of using sole RBIAS metric sometimes may be misleading because RBIAS value may be from the average of different error components with inverse signs [8]. For instance, the values of the NRMSE metric for the two corrected products (i.e., ILSF-RT and GSMaP-Gauge-NRT) are smaller than those of the GSMaP-NRT in the rain rates ranging from 1 mm hr^{-1} to 5 mm hr^{-1}. However, their RBIAS values are higher than those of GSMaP-NRT (see Fig. 8). Tian et al. [23] proposed an error decomposition technique to avoid above-mentioned situation. This technique is to separate the RBIAS into hit bias, miss bias, and false bias and is a fairer method to analyze and compare the performance of different precipitation products. In this study, this technique was used to compare the performance of the three products and answer the question of which error components are corrected by new

proposed method.

The spatial maps of the RBIAS and its three independent components (i.e., hit bias, miss bias, and false bias) for the three products over mainland China are given in Fig. 9. Overall, both the gauge-adjusted method used in GSMaP-Gauge-NRT and the new method significantly reduce the rainfall bias of the GSMaP-NRT over semi-humid areas. Especially, the new method remarkably reduces the rainfall bias in northeast China, central humid regions, and eastern coast areas where GSMaP-Gauge-NRT still has obvious overestimations. The lower total biases of ILSF-RT precipitation product mainly owe to the correction of hit component by new proposed method. One can see that the hit biases of ILSF-RT fall between -40% and 20% in most areas, suggesting that the new proposed method effectively reduces the hit biases (> 40%) of the GSMaP-NRT. However, there is minor improvements in the false and miss error components. One should be noted that the reduction of missed precipitation for satellite precipitation products needs to fuse rain gauge observations and other rainfall inputs to come true. In other words, both the error adjustment method employed in GSMaP-Gauge-NRT and the new proposed method (or existing other error correction methods, for example, Tian et al. [30]) cannot substantially reduce miss biases.

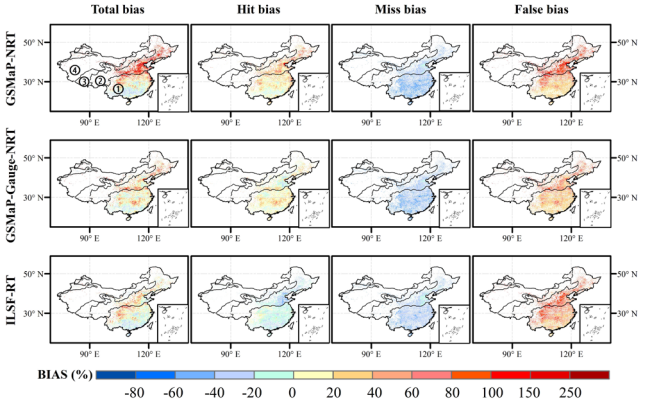

Fig. 9. Spatial maps of the total bias and its three components for the three products (i.e., GSMaP-NRT, GSMaP-Gauge-NRT, and ILSF-RT) at 0.1° spatial and hourly temporal resolution over mainland China for the validation period. Note that ①, ②, ③, and ④ represent humid, semi-humid, semi-arid, and arid type areas, respectively.

B. What are advantages and limitations of the new method?

Currently, most studies focused on the fusion of multi-source data (including ground-based observations, satellite information, and/or reanalysis data) to improve the quality of satellite precipitation estimates, such as GSMaP-Gauge [52], IMERG-Final [46], MSWEP [39], [40], and so on. These merged products have lower biases than those near real-time satellite precipitation estimates. However, they cannot be obtained in near real time mainly due to waiting for necessary rain gauge observations. Another issue is that the quality of these merged products relies on rain gauge observations to some extents. Compared with these merged methods, the new method proposed in this study has the advantages in that corrects the rainfall errors in real time without using real time obtaining rain gauge observations, and it can satisfy the requirement in high accuracy for the near real-time applications.

Given that the near real-time satellite precipitation estimates contain larger errors and uncertainties, GSMaP team has developed a gauge-adjusted GSMaP-NRT precipitation product, GSMaP-Gauge-NRT. Nevertheless, a preliminary evaluation executed by Lu and Yong, [50] found that GSMaP-Gauge-NRT still has large errors. Meanwhile, several studies have focused on investigating the real-time bias correction methods [30], [32]-[34], [37]. Tian et al. [30] proposed a Bayesian scheme to reduce the bias of satellite-based precipitation estimates in real time. Nevertheless, Bayesian scheme works for only reducing systematic errors, yet Chen et al. [8] pointed out that the total errors of satellite precipitation estimates are dominated by random errors. On the other hand, some literatures used satellite soil moisture data to reduce the errors of satellite precipitation estimates in near real time [33], [37]. However, these schemes might introduce the new error sources due to the large errors inherent in satellite soil moisture. Besides, some error adjustment models missed some crucial factors associated with errors [35], [36].

Compared with the error correction methods proposed in the above-mentioned literatures, the new proposed method entirely considers the relationships between retrieval errors and four crucial factors, which reduces the errors more effectively in theory. In practice, the new method substantially reduces the rainfall errors of the original GSMaP-NRT, and its product ILSF-RT shows better performance than GSMaP-Gauge-NRT. Meanwhile, the new method is designed to reduce the systematic and random errors existing in satellite precipitation estimates. More importantly, this method is rather substantial improvements in cold seasons (spring and winter) and over western China. The reduction in errors is limited for these seasons and these areas in previous studies [30], [37]. Additionally, our proposed method can solve the parameter estimates of EAMs without a large number of samples. Theoretically, the parameter estimates of each EAM can be derived using only three samples. For instance, the training samples are only 45 for the winter season in arid areas (see Fig. 2), the new method still significantly improves the accuracy of the GSMaP-NRT and its product performs the best among three products. Despite that the new method shows great advantages for error corrections in real time relative to existing real-time error correction methods, it also cannot reduce missed precipitation and is limited improvements in reducing false errors. In addition, this method has another common problem also inherent in the existing algorithms, that is, underestimating the rainfall volume in the rain rates over 1 mm hr^{-1}.

VI. CONCLUSION

In this study, we systematically investigated the relationships between the retrieval errors of satellite precipitation estimates and four crucial factors including topography, seasonality, climate type, and rain rate over mainland China. Based on the spatial plane function relationships adaptive for 16 different categories, we proposed a novel bias adjustment method to correct the hourly GSMaP-NRT estimates in real time. Last, we comprehensively evaluated the performance of new method by comparing the corrected satellite precipitation dataset ILSF-RT and original GSMaP product suite (i.e., GSMaP-NRT and

GSMaP-Gauge-NRT) over the entire mainland China. Results drawn from our analyses may be substantially benefit the GPM-based retrieval algorithms to produce more reliable and accurate satellite precipitation estimates for the satellite precipitation community. The major conclusions are summarized as follows:

Generally speaking, ILSF-RT product performs the best among three products in terms of RMSE, and RBIAS scores (see Table II), meaning that the new proposed method is effective for reducing the rainfall errors of original GSMaP-NRT. Meanwhile, the new method effectively reduces the errors of GSMaP-NRT associated with seasonality and climate (see Figs. 4-5). In particular, this new proposed method evidently improves the data quality over arid areas and cold seasons (spring and winter), which improves the application potentials of GSMaP-NRT in such areas where no ground observations are not available.

In spatial analysis, the new method improves the accuracy of the original GSMaP-NRT over most areas for both calibration and validation periods. In particular, the new method effectively reduces the errors of the original GSMaP-NRT over most areas of humid areas where the error correction method employed in GSMaP-Gauge-NRT degrades the accuracy of the original GSMaP-NRT in most cases. Notably, the new method evidently improves the accuracy of GSMaP-NRT for Sichuan province where has more mountainous terrains. That is due to the new proposed method comprehensively considering the relations between retrieval error and topography.

ILSF-RT shows the highest accuracy in all rain rates except for the total rain rates exceeding 5 mm/h. However, both new method and existing methods have a common issue, that is, increasing the degree of the underestimation in the rain rates over 1 mm hr^{-1}. This is due to the overcorrection of those methods for such rain rates.

An error decomposition technique was used to explore which error components are corrected by the new method. The results show that the new error correction method mainly corrects hit error component, whereas both error correction method used in GSMaP-Gauge-NRT and new method cannot correct the missed precipitation.

Overall, the new method proposed in this study considers the relationships between retrieval errors and four crucial factors, and the verification results have proved the effectiveness in reducing the retrieval errors. Looking into the ongoing GPM era, the new error correction method could be selected by algorithm developers as an important part of processing modules for GSMaP-Gauge-NRT, and meanwhile be used by end-users as a postprocessing step to improve the quality of satellite data before using satellite data for the near real-time hydrometeorological applications.

ACKNOWLEDGMENT

The authors would like to thank the JAXA precipitation team for providing GSMaP suite freely to the public. Also, we would like to express our most sincere thanks to the editor Dr. Simon Yueh and three anonymous reviewers for their efforts in enhancing the quality of this paper. This work was financially supported by the National Key Research and Development Program of China (No. 2018YFA0605402), the National Natural Science Foundation of China (Nos. 51979073 and 42074030), and the China Postdoctoral Science Foundation (No. 2021M700923).

REFERENCES

[1] C. Kidd, and G. J. Huffman, "Global precipitation measurement," Meteorol. Appl., vol. 18, pp. 334-353, Mar. 2011.

[2] A. Y. Hou, R. K. Kakar, S. Neeck, A. A. Azarbarzin, C. D. Kummerow, M. Kojima, R. Oki, K. Nakamura, and T. Lguchi, "The global precipitation measurement mission," Bull. Am. Meteorol. Soc., vol. 95, pp. 701-722, May, 2014.

[3] J. Wang, Y. Hong, L. Li, J. J. Gourley, S. I. Khan, K. K. Yilmaz, R. F. Adler, F. S. Policelli, S. Habib, D. Irwn, A. S. Limaye, T. Korme, and A. S. Limaye, "The coupled routing and excess storage (CREST) distributed hydrological model," Hydrol. Sci. J., vol. 56, pp. 84-98, Jan. 2011.

[4] H. Wu, R. F. Adler, Y. Tian, G. J. Huffman, H. Li, J. Wang, "Real-time global flood estimation using satellite-based precipitation and a coupled land surface and routing model," Water Resour. Res., vol. 50, pp. 2693-2717, Mar. 2014.

[5] B. Yong, D. Liu, J. J. Gourley, Y. Tian, G. J. Huffman, L. Ren, and Y. Hong, "Global view of real-time TRMM multisatellite precipitation analysis: Implications for its successor global precipitation measurement mission," Bull. Am. Meteorol. Soc., vol. 96, pp. 283-296, Feb. 2015.

[6] H. Chen, B. Yong, W. Qi, H. Wu, L. Ren, and Y. Hong, "Investigating the evaluation uncertainty for satellite precipitation estimates based on two different ground precipitation observation products," J. Hydrometeorol., vol. 21, pp. 2595-2606, Nov. 2020.

[7] H. Chen, B. Yong, Y. Shen, J. Liu, Y. Hong, and J. Zhang, "Comparison analysis of six purely satellite-derived global precipitation estimates," J. Hydrol., vol. 581, pp. 124376, Feb. 2020.

[8] H. Chen, B. Yong, P. E. Kirstetter, L. Wang, and Y. Hong, "Global component analysis of errors in three satellite-only global precipitation estimates," Hydrol. Earth Syst. Sci., vol. 25, pp. 3087-3104, Jun. 2021.

[9] A. AghaKouchak, A. Behrangi, S. Sorooshian, K. Hsu, and E. Amitai, "Evaluation of satellite retrieved extreme precipitation rates across the central United States," J. Geophys. Res.-Atmos., vol. 116, pp. D02115, Jan. 2011.

[10] B. Yong, L. Ren, Y. Hong, J. Wang, J. J. Gourley, S. Jiang, X. Chen, and W. Wang, "Hydrologic evaluation of Multisatellite Precipitation Analysis standard precipitation products in basins beyond its inclined latitude band: A case study in Laohahe basin, China," Water Resour. Res., vol. 46, pp. W07542, Jul. 2010.

[11] B. Yong, L. Ren, Y. Hong, J. J. Gourley, Y. Tian, G. J. Huffman, X. Chen, W. Wang, and Y. Wen, "First evaluation of the climatological calibration algorithm in the real-time TMPA precipitation estimates over two basins at high and low latitudes," Water Resour. Res., vol. 49, pp. 2461-2472, May, 2013.

[12] J. Tan, W. A. Petersen, P. E. Kirstetter, Y. Tian, "Performance of IMERG as a function of spatiotemporal scale," J. Hydrometeorol., vol. 18, pp. 307-319, Feb. 2017.

[13] S. Prakash, A. K. Mitra, A. AghaKouchak, Z. Liu, H. Norouzi, and D. S. Pai, "A preliminary assessment of GPM-based multi-satellite precipitation estimates over a monsoon dominated region," J. Hydrol., vol. 556, pp. 865-876, Jan. 2018.

[14] A. S. Gebregiorgis, P. E. Kirstetter, Y. Hong, J. J. Gourley, G. J. Huffman, W. A. Petersen, X. Xue, and M. R. Schwaller, "To what extent is the day 1 GPM IMERG satellite precipitation estimate improved as compared to TRMM TMPA-RT?," J. Geophys. Res.-Atmos., vol. 123, pp. 1694-1707, Mar. 2018.

[15] H. E. Beck, M. Pan, T. Roy, G. P. Weedon, F. Pappenberger, A. I. van Dijk, G. J. Huffman, R. F. Adler, and E. F. Wood, "Daily evaluation of 26 precipitation datasets using Stage-IV gauge-radar data for the CONUS," Hydrol. Earth Syst. Sci., vol. 23, pp. 207-224, Jan. 2019.

[16] Y. Tian, and C. D. Peters-Lidard, "A global map of uncertainties in satellite-based precipitation measurements," Geophys. Res. Lett., vol. 37, pp. L24407, Dec. 2010.

[17] H. E. Beck, N. Vergopolan, M. Pan, V. Levizzani, A. I. van Dijk, G. P. Weedon, L. Brocca, F. Pappenberger, G. J. Huffman, and E. F. Wood, "Global-scale evaluation of 22 precipitation datasets using gauge

observations and hydrological modeling," Hydrol. Earth Syst. Sci., vol. 21, pp. 6201-6217, Dec. 2017.

[18] F. A. Hirpa, M. Gebremichael, and T. Hopson, "Evaluation of High-Resolution Satellite Precipitation Products over Very Complex Terrain in Ethiopia," J. Appl. Meteorol. Climatol., vol. 49, pp. 1044-1051, May, 2010.

[19] C. Andermann, S. Bonnet, and R. Gloaguen, "Evaluation of precipitation data sets along the Himalayan front," Geochem. Geophys. Geosyst., vol. 12, pp. Q07023, Jul. 2011.

[20] Y. Gao, and M. Liu, "Evaluation of high-resolution satellite precipitation products using rain gauge observations over the Tibetan Plateau," Hydrol. Earth Syst. Sci., vol. 17, pp. 837-849, Feb. 2013.

[21] K. Takido, O. C. S. Valeriano, M. Ryo, K. Tanuma, T. Ushio, and T. Kubota, "Spatiotemporal evaluation of the gauge-adjusted global satellite mapping of precipitation at the basin scale," J. Meteorol. Soc. Jpn., vol. 94, pp. 185-195, Feb. 2016.

[22] T. Kubota, T. Ushio, S. Shing, S. Kida, M. Kachi, and K. Okamoto, "Verification of high-resolution satellite-based rainfall estimates around Japan using a gauge-calibrated ground-radar dataset," J. Meteorol. Soc. Jpn., vol. 87A, pp. 203-222, Mar. 2009.

[23] Y. Tian, C. D. Peters-Lidard, J. B. Eylander, R. J. Joyce, G. J. Huffman, R. F. Adler, K. L. Hsu, F. J. Turk, M. Garcia, and J. Zeng, "Component analysis of errors in satellite-based precipitation estimates," J. Geophys. Res.-Atmos., vol. 114, pp. D24101, Dec. 2009.

[24] H. Guo, A. Bao, F. Ndayisaba, T. Liu, A. Kurban, and P. De Maeyer, "Systematical evaluation of satellite precipitation estimates over central Asia using an improved error-component procedure," J. Geophys. Res. Atmos., vol. 122, pp. 10906. Oct. 2017.

[25] S. Moazami, S. Golian, Y. Hong, C. Sheng, M. R. Kavianpour, "Comprehensive evaluation of four high-resolution satellite precipitation products under diverse climate conditions in Iran," Hydrol. Sci. J.-J. Sci. Hydrol., vol. 61, pp. 420-440, Feb. 2016.

[26] Q. Zhu, W. Xuan, L. Liu, and Y. Xu, "Evaluation and hydrological application of precipitation estimates derived from PERSIANN-CDR, TRMM 3B42V7, and NCEP-CFSR over humid regions in China," Hydrol. Process., vol. 30, pp. 3061-3083, Mar. 2016.

[27] A. AghaKouchak, A. Mehran, H. Norouzi, and A. Behrangi, "Systematic and random error components in satellite precipitation data sets," Geophys. Res. Lett., Vol. 39, pp. L09406, May, 2012.

[28] V. Maggioni, M. R. Sapiano, and R. F. Adler, "Estimating Uncertainties in High-Resolution Satellite Precipitation Products: Systematic or Random Error?," J. Hydrometeorol., vol. 17, pp. 1119-1129, Apr. 2016.

[29] H. Chen, B. Yong, J. J. Gourly, J. Liu, L. Ren, W. Wang, Y. Hong, and J. Zhang, "Impact of the Crucial Geographical and Climatic Factors on the Input Source Errors of GPM-based Global Satellite Precipitation Estimates," J. Hydrol., vol. 575, pp. 1-16, Aug. 2019.

[30] Y. Tian, C. D. Peterslidard, and J. B. Eylander, "Real-Time Bias Reduction for Satellite-Based Precipitation Estimates," J. Hydrometeorol., vol. 11, pp. 1275-1285, Jun. 2010.

[31] P. Xie, and A. Xiong, "A conceptual model for constructing high-resolution gauge-satellite merged precipitation analyses," J. Geophys. Res., vol. 116, pp. D21106, Nov. 2011.

[32] Y. Shen, P. Zhao, Y. Pan, J. Yu, "A high spatiotemporal gauge-satellite merged precipitation analysis over China," J. Geophys. Res.-Atmos., vol. 119, pp. 3063-3075, Jun. 2014.

[33] W. Zhan, M. Pan, N. Wanders, and E. F. Wood, "Correction of real-time satellite precipitation with satellite soil moisture observations," Hydrol. Earth Syst. Sci., vol. 19, pp. 4275-4291, Oct. 2015.

[34] Z. Yang, K. Hsu, S. Sorooshian, X. Xu, D. Braithwaite, and K, M. J. Verbist, "Bias adjustment of satellite-based precipitation estimation using gauge observations: A case study in Chile," J. Geophys. Res.-Atmos., vol. 121, pp. 3790-3806, Aug. 2016.

[35] H. Hashemi, M. Nordin, V. Lakshmi, G. J. Huffman, and R. Knight, "Bias Correction of Long-Term Satellite Monthly Precipitation Product (TRMM 3B43) over the Conterminous United States,". J. Hydrometeorol., vol. 18, pp. 2491-2509, Sep. 2017.

[36] H. M. Le, J. R. Sutton, D. Du Bui, J. D. Bolten, V. Lakshmi, "Comparison and Bias Correction of TMPA Precipitation Products over the Lower Part of Red-Thai Binh River Basin of Vietnam," Remote Sens., vol. 10, pp. 1582, Oct. 2018.

[37] Z. Zhang, D. Wang, G. Wang, J. Qiu, and W. Liao, "Use of SMAP Soil Moisture and Fitting Methods in Improving GPM Estimation in Near Real Time,". Remote Sens., vol. 11, pp. 368, Mar. 2019.

[38] X. Lu, G. Tang, X. Wang, Y. Liu, L. Jia, G. Xie, S. Li, and Y. Zhang, "Correcting GPM IMERG precipitation data over the Tianshan Mountains in China," J. Hydrol., vol. 575, pp. 1239-1252, Aug. 2019.

[39] H. E. Beck, A. I. Van Dijk, V. Levizzani, J. Schellekens, D. G. Miralles, B. Martens, A. De Roo, "MSWEP: 3-hourly 0.25° global gridded precipitation (1979-2015) by merging gauge, satellite, and reanalysis data," Hydrol. Earth Syst. Sci., vol. 21, pp. 589-615, Jan. 2017.

[40] H. E. Beck, E. F. Wood, M. Pan, C. K. Fisher, D. G. Miralles, A. I. Van Dijk, T. R. McVicar, and R. F. Adler, "MSWEP V2 Global 3-Hourly 0.1° Precipitation: Methodology and Quantitative Assessment,". Bull. Amer. Meteorol. Soc., vol. 100, pp. 473-500, Mar. 2019.

[41] G. Shen, N. Chen, W. Wang, and Z. Chen, "WHU-SGCC: a novel approach for blending daily satellite (CHIRP) and precipitation observations over the Jinsha River basin," Earth Syst. Sci. Data., vol. 11, pp. 1711-1744, Apri. 2019.

[42] O. M. Baez-Villanueva, M. Zambrano-Bigiarini, H. E. Beck, I. McNamara, L. Ribbe, A. Nauditt, C. Birkel, K. Verbist, J. D. Giraldo-Osorio, and N. X. Thinh, "RF-MEP: A novel random forest method for merging gridded precipitation products and ground-based measurements," Remote Sens. Environ., vol. 239, pp. 111606, Mar. 2020.

[43] Z. Ma, J. Xu, S. Zhu, J. Yang, G. Tang, Y. Yang, Z. Shi, and Y. Hong, "AIMERG: a new Asian precipitation dataset (0.1°/half-hourly, 2000-2015) by calibrating the GPM-era IMERG at a daily scale using APHRODITE," Earth Syst. Sci. Data., vol. 12, pp. 1525-1544, Mar. 2020.

[44] T. Kubota, S. Shige, H. Hashizume, K. Aonashi, N. Takahashi, S. Seto, M. Hirose, Y. N. Takayabu, T. Ushio, K. Nakagawa, K. Iwanami, M. Kachi, K. Okamoto, "Global precipitation map using satellite-borne microwave radiometers by the GSMaP project: Production and validation," IEEE Trans. Geosci. Remote Sensing., vol. 45, pp. 2259-2275, Jul. 2007.

[45] T. Ushio, K. Sasashige, T. Kubota, S. Shige, K. I. Okamoto, K. Aonashi, T. Inoue, N. Takahashi, T. Iguchi, M. Kachi, R. Oki, T. Morimoto, and Z. I. Kawasaki, "A Kalman filter approach to the Global Satellite Mapping of Precipitation (GSMaP) from combined passive microwave and infrared radiometric data," J. Meteorol. Soc. Jpn. Ser. II, vol. 87A, pp. 137-151, Feb. 2009.

[46] G. J. Huffman, D. T. Bolvin, D. Braithwaite, K. Hsu, R. Joyce, C. Kidd, E. J. Nelkin, S. Sorooshian, J. Tan, and P. Xie, "Algorithm Theoretical Basis Document (ATBD) version 06. NASA Global Precipitation Measurement (GPM) Integrated Multi-satellitE Retrievals for GPM (IMERG) (Algorithm Theoretical Basis Document)," pp. 38, 2019.

[47] S. Sorooshian, K. L. Hsu, X. Gao, H. V. Gupta, B. Imam, and D. Braithwaite, "Evaluation of PERSIANN system satellite-based estimates of tropical rainfall," Bull. Am. Meteorol. Soc., vol. 81, pp. 2035-2046, Sep. 2000.

[48] Y. Hong, K. L. Hsu, S. Sorooshian, and X. Gao, "Precipitation estimation from remotely sensed imagery using an artificial neural network cloud classification system," J. Appl. Meteorol., vol. 43, pp. 1834-1853, Dec. 2004.

[49] P. Xie, M. Chen, S. Yang, A. Yatagai, T. Hayasaka, Y. Fukushima, and C. Liu, "A gauge-based analysis of daily precipitation over East Asia,". J. Hydrometeorol., vol. 8, pp. 607-626, Mar. 2007.

[50] D. Lu, and B. Yong, "A Preliminary Assessment of the Gauge-Adjusted Near-Real-Time GSMaP Precipitation Estimate over Mainland China," Remote Sens., vol. 12, pp.141, Jan. 2020.

[51] P. C. Hansen, and D. P. Oleary, "The use of the L-curve in the regularization of discrete ill-posed problems," SIAM J. Sci. Comput., vol. 14, pp. 1487-1503. Jun. 1993.

[52] T. Mega, T. Ushio, M. Takahiro, T. Kubota, M. Kachi, and R. Oki, "Gauge-Adjusted Global Satellite Mapping of Precipitation," IEEE Trans. Geosci. Remote Sensing, vol. 57, pp. 1928-1935, Apr. 2019.